INTERNAL MEDICINE

□ CASE REPORT □

^{11}C-PiB PET Imaging of Encephalopathy Associated with Cerebral Amyloid Angiopathy

Renpei Sengoku[1,2], Satoshi Matsushima[3], Yoshitake Murakami[4], Takahiro Fukuda[5], Aya M. Tokumaru[6], Masaya Hashimoto[1], Masahiko Suzuki[1], Kiichi Ishiwata[7], Kenji Ishii[7] and Soichiro Mochio[8]

Abstract

We herein report that the clinical, laboratory, and radiographic features and positron emission tomography (PET) imaging may provide valuable clues to the pathogenesis of cerebral amyloid angiopathy (CAA)-associated encephalopathy, which currently remains unclear. We herein describe two cases of encephalopathy with CAA, with an emphasis on PET imaging with ^{11}C-Pittsburgh compound B (^{11}C-PiB) and ^{18}F-fluorodeoxyglucose (^{18}F-FDG). One case of Alzheimer's disease for which a brain biopsy was performed showed CAA-related inflammation. Another case that had developed sudden sensory aphasia presented with posterior reversible encephalopathy syndrome-like vasogenic edema in the left temporal region with ^{11}C-PiB uptake and microhemorrhages. ^{11}C-PiB and ^{18}F-FDG PET are useful for detecting CAA-associated encephalopathy, including atypical CAA cases.

Key words: cerebral amyloid angiopathy, vasogenic edema, PET, sensory aphasia, hemodialysis

(Intern Med 53: 1997-2000, 2014)
(DOI: 10.2169/internalmedicine.53.1731)

Introduction

Cerebral amyloid angiopathy (CAA) characteristically shows localized amyloid deposition in cerebral blood vessels, including the small- and medium-sized arteries of the leptomeninges and superficial cortex. The clinical manifestations of CAA include leukoencephalopathy or encephalopathy (1, 2). T2* weighted images (WI) or susceptibility-weighted images (SWI) can detect microbleeding to provide support for a diagnosis of CAA (3, 4). SWI can identify many more microhemorrhages than conventional T2*WI magnitude techniques (5). A recent study described the correlation of SWI focal intensities to tissue pathology in post mortem human CAA-affected brain (6). We herein present two cases of encephalopathy with CAA, one with a clinical course of Alzheimer's disease (AD) modified by CAA-related inflammation, and another with atypical initial manifestations of CAA. We describe the findings with an emphasis on positron emission tomography (PET) imaging with ^{11}C-Pittsburgh compound B (^{11}C-PiB) and ^{18}F-fluorodeoxyglucose (^{18}F-FDG).

Case Reports

Case 1

A 72-year-old man presented with hypertension and a history of cognitive decline that manifested at the age of 65 and gradually progressed until he was 71 years old, when it accelerated. His caregiver described that he suffered from memory disturbances; for example, he was unable to find

[1]Department of Neurology, The Jikei University School of Medicine, Japan, [2]Department of Neurology, Tokyo Metropolitan Geriatric Hospital, Japan, [3]Department of Radiology, The Jikei University School of Medicine, Japan, [4]Department of Neurology, Saiseikai Kurihashi Hospital, Japan, [5]Department of Neuropathology, The Jikei University School of Medicine, Japan, [6]Department of Diagnostic Radiology, Tokyo Metropolitan Medical Center of Gerontology, Japan, [7]Positron Medical Center, Tokyo Metropolitan Institute of Gerontology, Japan and [8]The Jikei University School of Nursing, Japan
Received for publication September 8, 2013; Accepted for publication March 4, 2014
Correspondence to Dr. Renpei Sengoku, renpei_sengoku@tmghig.jp

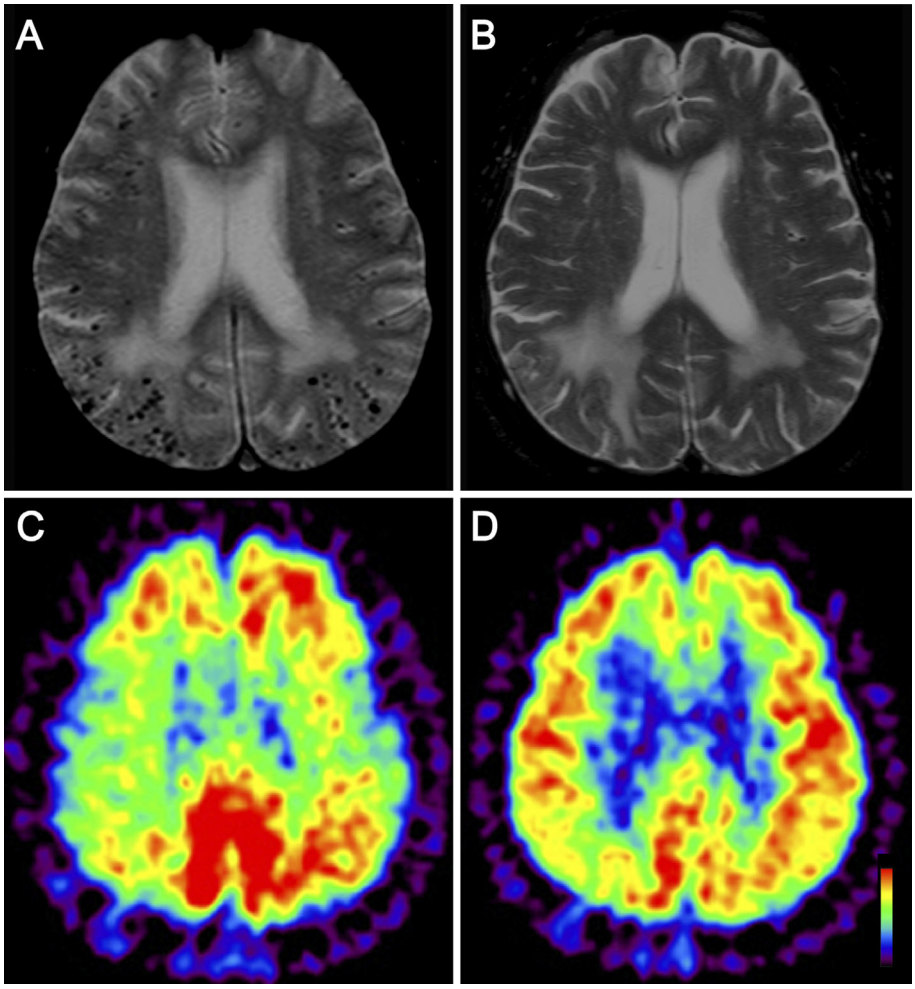

Figure 1. **MRI and PET scans of Case 1. A: Brain MRI showed cortical and subcortical microbleeds on T2*WI, predominantly in the dorsal portion of the bilateral temporo-parieto-occipital lobes. B: Axial brain MRI T2*WI exhibited a high-intensity area (HIA) in the right temporo-parieto-occipital white matter with edema. C: ^{11}C-PiB-PET showed accumulation in the fronto-parieto-temporal lobe and precuneus in an AD-like pattern. D: ^{18}F-FDG-PET revealed hypometabolism in the right temporo-parieto-occipital lesion.**

his way home after trips outside. He was admitted to our hospital after exhibiting wandering behavior for one month. An examination revealed acute progressive dementia and spatial disorientation. He became disinhibited, urinated on the ward, and removed his intravenous drip soon after insertion. His plantar responses were flexor bilaterally, and there were no extra-pyramidal signs. The patient's Mini-Mental State Examination score was 16/30. He had been taking 50 mg atenolol and 5 mg amlodipine for hypertension and 5 mg pravastatin for several years. His cerebrospinal fluid (CSF) cell counts and protein and glucose levels were within normal ranges. The patient's brain magnetic resonance imaging (MRI) scan taken on admission showed multiple cerebral microbleeds on T2*WI, predominantly in the dorsal portion of bilateral temporo-parieto-occipital lobes (Fig. 1A). T2*WI revealed a high-intensity area (HIA) in the right temporo-parieto-occipital white matter with edema (Fig. 1B). An excisional biopsy from the right parieto-occipital lobe was performed. A neuropathological examination revealed severe amyloid deposits in the cortical and leptomeningeal blood vessel walls (Fig. 2). This specimen revealed quite a few neurofibrillary tangles and neuropil threads and numerous senile plaques (Fig. 2). An inflammatory perivascular infiltrate was also observed (Fig. 2). He was given intravenous steroid pulse therapy and dexamethasone. HIAs improved on T2*WI and fluid-attenuated inversion recovery (FLAIR) imaging, although irreversible changes remained. Static emission data were acquired for 45-51 min and 40-70 min after intravenous bolus injections of ^{18}F-FDG and ^{11}C-PiB, respectively. ^{11}C-PiB-PET accumulated in the fronto-parieto-temporal lobe and precuneus in an AD-like pattern (Fig. 1C) (7, 8). ^{18}F-FDG-PET revealed hypometabolism in the right temporo-parieto-occipital lesion (Fig. 1D). The patient was homozygous for the ε4 allele of the apolipoprotein E gene (*APOE*).

Case 2

A right-hand-dominant, 72-year-old man receiving hemodialysis for membranous nephropathy noticed an inability to write his address correctly one day after hemodialysis. He

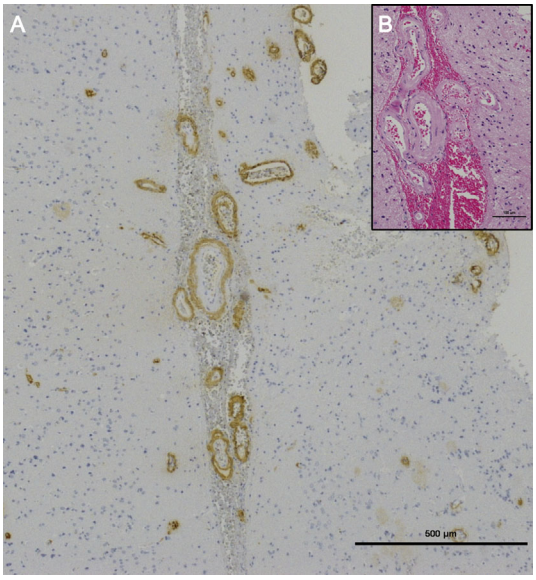

Figure 2. Neuropathological findings in Case 1. A: Brain biopsy specimen: immunocytochemistry for β-amyloid revealed severe amyloid deposits in the cortical and leptomeningeal blood vessel walls (scale bar=500 μm). B: Hematoxylin and Eosin staining showed thickening and hyalinization of the subarachnoid and intracortical blood vessels (scale bar=100 μm).

reported that he could not understand his own speech in Japanese. Interestingly, he tried to speak in English, and he could not understand what he said. A neurological examination revealed sensory aphasia. His systolic blood pressure was 190 mmHg. The patient's serum blood urea nitrogen, creatinine, and uric acid levels were 72 mg/dL, 12.8 mg/dL, and 8.5 mg/dL, respectively. His CSF laboratory values were 2.6 white blood cells/mm^3, 147 mg/dL protein, and 52 mg/dL glucose, and his CSF amyloid β1-42 protein level was <25 pmol/L. The patient's brain MRI showed HIA in the left temporal cortex on FLAIR (Fig. 3A). There was no HIAs on diffusion-weighted imaging. SWI revealed low-intensity areas in these regions and in the subarachnoid space (Fig. 3B). He received antihypertensive treatment without steroids or immunosuppressive drugs, and his symptoms completely resolved. A subsequent MRI revealed no HIA, and posterior reversible encephalopathy syndrome (PRES)-like changes were observed in the superior temporal gyrus. PET was performed to detect amyloid deposits 10 months after onset. ^{11}C-PiB-PET showed focal uptake in the left temporal lobe (Fig. 3C). The regional uptake lesion observed on amyloid PET imaging corresponded to subarachnoid hemosiderosis and microbleeds, especially in the cortical and subcortical area of the left temporal lobes. We suggest that this focal uptake lesion was indicative of amyloid angiopathy. The low ^{18}F-FDG uptake was not in an AD-like distribution; rather, it was only present in the left temporal region (Fig. 3D).

Discussion

We presented two cases of encephalopathy with CAA, one with a clinical course of AD modified by CAA-related inflammation, and another with atypical initial manifestations of CAA. The symptoms leading to admission were acute encephalopathy associated with CAA as demonstrated by ^{11}C-PiB-PET and MRI. One case was neuropathologically confirmed following a brain biopsy. These two cases suggest that CAA encephalopathy might be mediated by underlying inflammation and shares similar features with PRES.

In case 1, AD had been diagnosed two years previously. An MRI revealed numerous microbleeds, and the patient's brain biopsy showed senile plaques (AD pathology) with perivascular inflammatory changes. The specimen also exhibited fibrinoid necrosis of a parenchymal arteriole. PET showed a remarkable AD-like pattern of ^{11}C-PiB and ^{18}F-FDG uptake. Case 1 was homozygous for APOE ε4, and steroids and immunosuppressive therapy were partially effective. Given the above findings, this case was considered to involve CAA-related inflammation (2, 4). The pathogenesis of CAA in case 1 apparently involved vasogenic edema and ischemic changes or gliosis associated with underlying AD pathology.

Case 2 presented with acute onset sensory aphasia coexisting with unstable hypertension secondary to chronic renal failure. A MRI scan showed HIA in the left superior temporal gyrus on T2*WI, and apparent diffusion coefficient mapping revealed vasogenic edema. SWI detected many microbleeds in the area corresponding to the lesion observed on FLAIR/T2WI. Although the investigations showed mild ^{11}C-PiB accumulation and focal hypometabolism atypical AD, ^{11}C-PiB uptake was observed in lesions with microbleeding, such as those in the left superior temporal gyrus. We considered the following in differential diagnoses: hypertensive vasculopathy, vascular malformation, PRES, and CAA. Brain microbleeds associated with hypertensive vasculopathy tend to be localized in the basal ganglia, internal capsule, brain stem, and cerebellum, whereas those associated with CAA are generally smaller with a posterior lobar predilection (6). Because we did not perform conventional digital subtraction angiography (9), we cannot completely rule out a vascular malformation; however, we do not strongly suspect this disorder. The patient's sensory aphasia fully resolved after antihypertensive therapy, and steroids were unnecessary. Although the patient's hypertensive state influenced the clinical symptoms, the findings of ^{11}C-PiB PET and SWI were suggestive of CAA. Similarly, the presence of cortical or subcortical microbleeds and old subarachnoid hemorrhage on MRI supported a diagnosis of CAA (8). The important point from this case is that the ^{11}C-PiB uptake lesions corresponded with the microbleeds observed on SWI scans. The patient's sensory aphasia likely occurred due to the lesion in the left superior temporal gyrus. His symptoms might have been caused by PRES-like focal vasogenic edema near vessels that were made vulnerable by amyloid deposition. Some authors suggest that amyloid angiopathy can alter vascular reactivity, leading to dysautoregulation and altered blood-brain barrier integ-

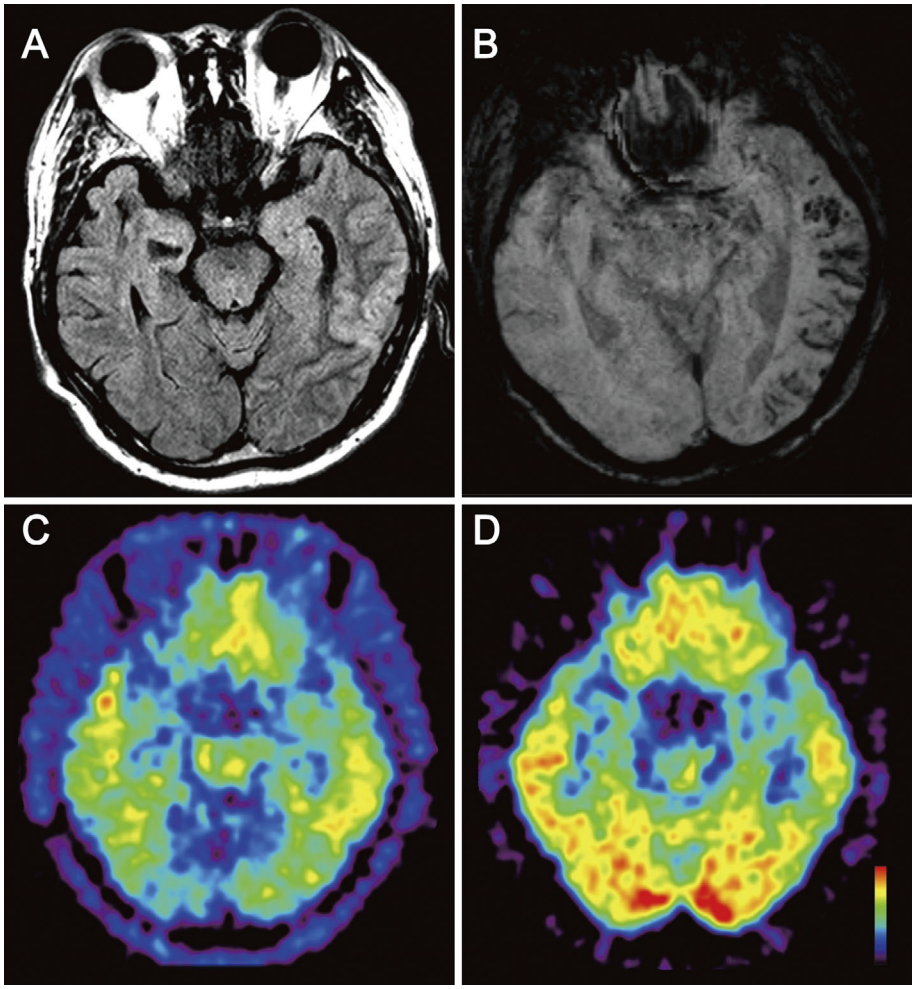

Figure 3. MRI and PET scans of Case 2. A: Brain MRI showed HIA in the left temporal cortex on FLAIR. B: SWI revealed low-intensity areas representing old hemorrhages in these regions and the subarachnoid space. C: ^{11}C-PiB-PET showed focal uptake in the left temporal lobe. D: Low ^{18}F-FDG uptake was not in an AD-like distribution; rather, it was only observed in the left temporal region.

rity (10).

In conclusion, the ^{11}C-PiB PET findings in these two cases supported diagnoses of CAA encephalopathy. We suggest that amyloid imaging is a useful diagnostic tool for investigating atypical clinical courses of patients with CAA.

The authors state that they have no Conflict of Interest (COI).

References

1. Gray F, Dubas F, Roullet E, Escourolle R. Leukoencephalopathy in diffuse hemorrhagic cerebral amyloid angiopathy. Ann Neurol **18**: 54-59, 1985.
2. Eng JA, Frosh MP, Choi K, Rebeck GW, Greenberg SM. Clinical manifestations of cerebral amyloid angiopathy-related inflammation. Ann Neurol **55**: 250-256, 2004.
3. Knudsen KA, Rosand J, Karluk D, Greenberg SM. Clinical diagnosis of cerebral amyloid angiopathy: validation of the Boston criteria. Neurology **56**: 537-539, 2001.
4. Kinnecom C, Lev MH, Wendell L, et al. Course of cerebral amyloid angiopathy-related inflammation. Neurology **68**: 1411-1416, 2007.
5. Haacke EM, DelProposto ZS, Chaturvedi S, et al. Imaging cerebral amyloid angiopathy with susceptibility-weighted imaging. Am J Neuroradiol **28**: 316-317, 2007.
6. Schrag M, McAuley G, Pomakian J, et al. Correlation of hypointensities in susceptibility-weighted images to tissue histology in dementia patients with cerebral amyloid angiopathy: a postmortem MRI study. Acta Neuropathol **119**: 291-302, 2010.
7. Johnson KA, Gregas M, Becker JA, et al. Imaging of amyloid burden and distribution in cerebral amyloid angiopathy. Ann Neurol **62**: 229-234, 2007.
8. Ly JV, Donnan GA, Villemagne VL, et al. 11C PiB binding is increased in patients with cerebral amyloid angiopathy-related hemorrhage. Neurology **74**: 487-493, 2010.
9. Lummel N, Lutz J, Bruckmann H, Linn J. The value of magnetic resonance imaging for the detection of the bleeding source in non-traumatic intracerebral haemorrhages: a comparison with conventional digital subtraction angiography. Neuroradiology **54**: 673-680, 2012.
10. Oh U, Gupta R, Krakauer JW, Khandji AG, Chin SS, Elkind MSV. Reversible leukoencephalopathy associated with cerebral amyloid angiopathy. Neurology **62**: 494-497, 2004.